Thermophoretic Forces on DNA Measured with a Single-Molecule Spring Balance

Jonas N. Pedersen, Christopher J. Lüscher, Rodolphe Marie, Lasse H. Thamdrup,* Anders Kristensen, and Henrik Flyvbjerg†

Department of Micro- and Nanotechnology, Technical University of Denmark, DK-2800 Lyngby, Denmark

(Received 7 July 2014; published 30 December 2014)

We stretch a single DNA molecule with thermophoretic forces and measure these forces with a spring balance: the DNA molecule itself. It is an entropic spring which we calibrate, using as a benchmark its Brownian motion in the nanochannel that contains and prestretches it. This direct measurement of the thermophoretic force in a static configuration finds forces up to 130 fN. This is eleven times stronger than the force experienced by the same molecule in the same thermal gradient in bulk, where the molecule shields itself. Our stronger forces stretch the middle of the molecule up to 80% of its contour length. We find the Soret coefficient per unit length of DNA at various ionic strengths. It agrees, with novel precision, with results obtained in bulk for DNA too short to shield itself and with the thermodynamic model of thermophoresis.

DOI: 10.1103/PhysRevLett.113.268301 PACS numbers: 82.35.Lr, 82.37.Rs, 87.14.gk

Thermophoresis, also known as the Ludwig-Soret effect, is the migration of particles along temperature gradients. In gases, this phenomenon is understood with kinetic gas theory [1]. Its microscopic origin in liquids is debated. Experiments have probed the thermophoretic properties of various colloidal suspensions—such as aqueous solutions of DNA, RNA, micelles, and polystyrene beads—and investigated their dependence on size, temperature, salt type, and salt concentration [2–7]. Individual DNA molecules have also been tethered and stretched [8]. Bulk observations agree on a crucial dependence on solvent-particle interactions [9], and theoretical models exist. They are based on either equilibrium thermodynamics [4,5,7,10], a hydrodynamic description [11–13], or fluctuating hydrodynamics [14], but no microscopic theory is generally accepted [9,15]. These fundamental issues and possible applications motivate a microfluidic interest in thermophoresis [16–20].

Individual DNA molecules can be manipulated and stretched in a nanofluidic device using light-induced local heating (LILH) [21]. Here, we study thermophoretic forces on individual DNA molecules quantitatively. Specifically, we measure the Soret coefficient per unit length of DNA, s_T, and its salt dependence. We prestretch a DNA molecule to ~30% of its contour length by flowing it into a nanochannel with a $200 \times 250\ \mathrm{nm}^2$ cross section. There, we grab its two halves with temperature gradients that pull them apart. The midregion is consequently stretched up to 80% of its contour length (Figs. 1 and 2). This degree of stretching is our first result and may be of practical interest; see the final paragraph.

Our experiment provides a new window on the nature of thermophoresis. Existing techniques measure the thermophoretic force from single-particle tracking or from changes in particle concentration, thus, balancing the thermophoretic force with hydrodynamic drag or entropic force [9]. In the latter case, a region with nonconstant temperature, $T(x)$, gives rise to a position-dependent equilibrium concentration $c(x)$

$$c(x) = c_0 e^{-S_T[T(x)-T_0]}, \tag{1}$$

where c_0 is the concentration of particles found where the temperature is T_0, and S_T is the Soret coefficient. In contrast, we measure the thermophoretic forces experienced by a single DNA molecule in a static configuration. These forces are read off the observed stretching of the DNA molecule using a simple linear-response theory. This theory predicts a local DNA density of the same form as Eq. (1), see Eq. (6), and it describes experimental observations accurately; see Fig. 2. This theory is our second result. Its parameters are determined at various ionic strengths (Fig. 3), including s_T (Fig. 4). The salt dependence of s_T is consistent with the thermodynamic model of thermophoresis [4,7]. This is our third result.

Experiment.—For fabrication of the nanofluidic chip in polymethylmethacrylate (PMMA), setup for LILH, and visualization of DNA, see [21]. Experiments were conducted on T4 DNA (166 kb, Nippon Gene) fluorescently dyed with YOYO-1 (Invitrogen) at a ratio of one dye molecule per five base pairs, and suspended in a loading buffer [22].

Temperature profiles in nanochannels were measured with the temperature-dependent fluorescent complex $[\mathrm{Ru(bpy)_3}]^{2+}$ [25]. The warm spot formed by the laser beam in the near-infrared (NIR) absorber layer [Fig. 1(a)] gave a temperature profile that is perfectly fitted by

$$T(x,y) = T_\infty + \frac{\Delta T_{\max} z_0}{\sqrt{(x-x_0)^2 + (y-y_0)^2 + z_0^2}}, \tag{2}$$

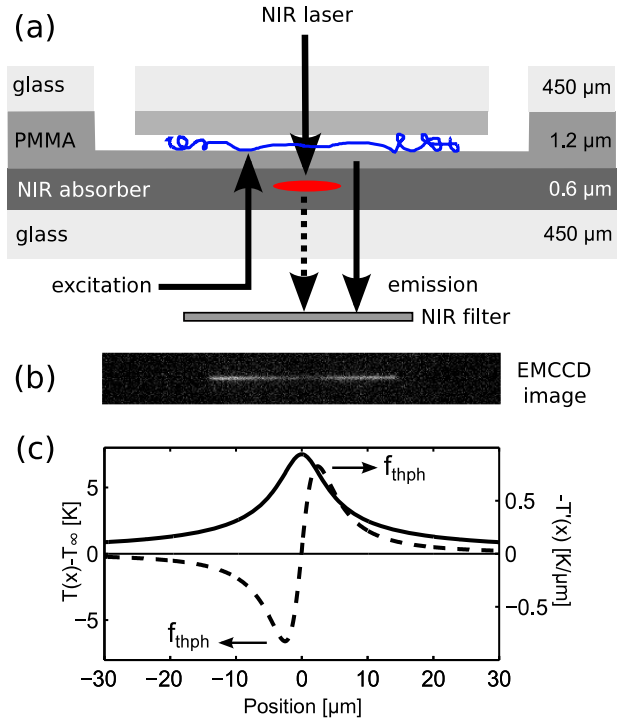

FIG. 1 (color online). Epifluorescence setup with NIR laser. (a) Layers of the chip with thicknesses indicated. The laser is focused on the absorber layer, creating a heated (red) spot. (b) A single fluorescent T4 DNA molecule conned in a nanochannel, imaged with an electron-multiplying charge-coupled device (EMCCD). It is stretched at its midregion by thermophoretic forces. (c) Temperature profile $T(x) - T_\infty$ (full line) and $-T'(x)$ (dashed line) stretching the molecule in (b). The force density, f_{thph}, indicated with arrows, is assumed proportional to $-T'(x)$.

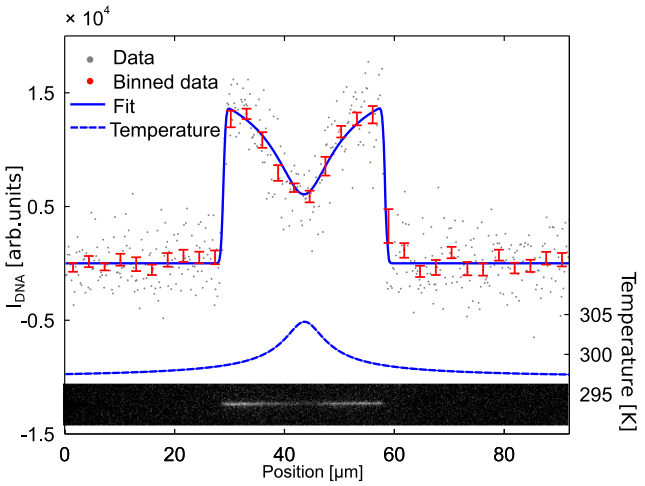

FIG. 2 (color online). Fluorescence intensity profile of thermophoretically stretched DNA molecule and temperature profile that stretched it. Bottom: One frame from movie of stretched molecule. Middle: Temperature profile used for stretching [Eq. (2)] (dashed blue curve). Top: Intensity $\mathcal{I}(x)$, a time average over 10 frames from movie (grey points). Further noise reduction, by bin averaging, gives $\bar{\mathcal{I}}(x)$ (red points). Fitted theoretical profile $\mathcal{I}_{\text{th}}(x) \propto \mathcal{D}(x)$ [Eq. (6)] (blue curve). This fit, to data points from the DNA plus a 2.6 μm margin of background at both ends, has a P value equal to 0.47.

where the z axis is parallel to the laser beam and optical axis of the microscope, while the (x, y) plane coincides with the array of nanochannels, the x axis being parallel to the channels. The function $T(x, y)$ above is the restriction to the (x, y) plane of the steady-state solution to the heat equation in a 3D homogeneous medium with a spherically symmetric source of heat at (x_0, y_0, z_0). It is also an excellent approximation to the solution obtained for our 2D Gaussian heat source with standard deviation σ located parallel to the (x, y) plane at (x_0, y_0, z_*), provided $z_0^2 = z_*^2 + 2\sigma^2$ [25]. Fitted values are $z_0 = 3.5$ μm, $\Delta T_{\text{max}} = 7.5$ K, and $T_\infty = T_{\text{room}} + 0.4$ K [25]. T_∞ is a little larger than room temperature because of the lower heat conductivity of the chip's surroundings. From here, $T(x)$ is shorthand for $T(x, 0)$.

The opposing thermal forces shown in Fig. 1(c) stretch the DNA to a quasiequilibrium configuration shown in Figs. 1(b) and 2. We filmed this configuration at 10 frames/s to monitor quasiequilibrium. Figure 1(b) shows the nature of the resulting data: a bright fluorescent strip with a width twice the channel width due to diffraction, and along its length, a variation in intensity that is proportional to the local concentration of DNA in the channel, smoothed by diffraction.

Model.—The simplest possible model that might capture the nature of our data, has only features that are seen in our data. Because of its simplicity, such a model is not easily fitted to data: It either fits or not, which makes it a more convincing model when it does. To achieve this convincing simplicity, we model the DNA in the channel as a one-dimensional homogeneous medium with linear elastic properties.

Let $\mathcal{D}(x)$ denote the local density of DNA, defined as DNA contour length per unit length of channel. Let $\mathcal{D}_0$ denote the equilibrium density at constant temperature. This density is maintained locally by a restoring entropic force: $\mathcal{D}(x) \neq \mathcal{D}_0$ causes a local tension, $\tau(x)$, in the medium. We assume linear response

$$\tau(x) = -\kappa[\mathcal{D}(x) - \mathcal{D}_0], \tag{3}$$

motivated by the mathematical advantages that a linear theory offers and the fact that any correct theory must be linear for sufficiently small differences $\mathcal{D}(x) - \mathcal{D}_0$. Here, κ is a coefficient of elasticity, and the restoring force (per unit length of channel) consequently is

$$f_{\text{entrp}}(x) = \tau'(x) = -\kappa\mathcal{D}'(x). \tag{4}$$

This linear response is sufficient to capture the nature of our data, we shall see [33].

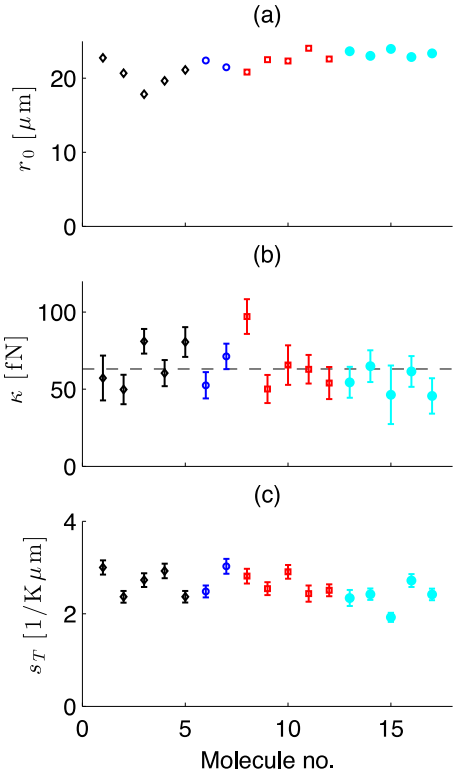

FIG. 3 (color online). Fitted values for model parameters. (a) Equilibrium length $r_0 \propto 1/\mathcal{D}_0$, (b) spring constant κ, and (c) thermophoretic coefficient s_T measured at four ionic strengths; (diamond) $I = 8$ mM, (open circle) $I = 14$ mM, (square) $I = 34$ mM, and (closed circle) $I = 75$ mM, respectively. Error bars are standard errors on the means. Errors on the equilibrium lengths r_0 are less than 2% of the values themselves. Dashed line shows weighted average.

The local force on the DNA (per unit length of channel) is assumed proportional to the amount, $\mathcal{D}(x)$, of DNA present and to the temperature gradient

$$f_{\text{thph}}(x) = -k_B T s_T T'(x) \mathcal{D}(x), \tag{5}$$

where the Soret coefficient, s_T, per unit contour length of DNA is assumed constant over the temperature range of the experiment, which is 8 °K.

In equilibrium, f_{entrp} and f_{thph} balance each other everywhere. Consequently,

$$\mathcal{D}(x) = \mathcal{D}_0 e^{-s_T (k_B T/\kappa)[T(x) - T(x_{\max})]} \tag{6}$$

for $-x_{\max} < x < x_{\max}$, and zero elsewhere. Here, we used boundary conditions $\mathcal{D}(\pm x_{\max}) = \mathcal{D}_0$ at the ends of the 1D medium, because (i) the ends remain in equilibrium, and (ii) $\mathcal{D}_0$ effectively is the same at T_{room} and at $T(\pm x_{\max})$, as these temperatures differ only ~1%.

This density profile was convoluted with a Gaussian that mimics the point-spread function of the microscope, then fitted to data. The only fit parameter was s_T, because $\mathcal{D}_0$ and κ were measured independently in advance, at constant temperature, T_{room}, with κ deduced from the Brownian fluctuations of the extent of the molecule in the nanochannel [25].

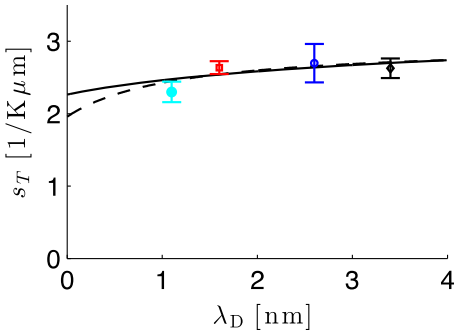

FIG. 4 (color online). Salt dependence of the thermophoretic coefficient. Same data as in Fig. 3(c). Full and dashed lines are fits to Eqs. (7) and (8), respectively, plus a constant offset $s_T^{(\text{off})}$. Error bars are standard errors on the means.

Data analysis.—The intensity profile $\mathcal{I}(x)$ was read off individual frames and time averaged over ten consecutive frames to reduce Brownian density fluctuations in the intensity profile. Figure 2 shows such a profile and a fit of our theory to it. The fitted constant of proportionality between density and intensity contains no information of interest. Neither does the fitted location x_0, while the fitted value for s_T determines both the length and the shape of the density profile.

Results.—Figure 3 summarizes results. For ionic strengths $I = 8$, 14, 34, 75 mM, the Debye layer around the DNA is approximately $\lambda_D = 3.4$, 2.6, 1.6, and 1.1 nm, respectively; see below. This is much smaller than the width of the nanochannels, but comparable to the DNA's radius $R_{\text{DNA}} = 1$ nm. Reisner *et al.* investigated how the equilibrium length of DNA in (glass) nanochannels depends on ionic strength [34]. For channel dimensions and ionic strengths similar to ours, they observed only a weak dependence. Figure 3(a) agrees with this.

Figure 3(b) shows that κ does not depend on ionic strength, in agreement with its entropic nature and the insignificance of excluded volume effects. Consequently, we use its weighted average $\kappa = 62 \pm 3$ fN below.

Figure 3(c) shows the thermophoretic coefficient obtained from fits to the density profile [Eq. (6); Fig. 2]. The same data are plotted versus Debye length in Fig. 4, which is our main quantitative result.

The forces add up along each half of the DNA molecule to a tension at its middle of $F_{\text{total}} = \kappa \mathcal{D}_0 (1 - \exp\{s_T (k_B T/\kappa)[T(0) - T(x_{\max})]\})$. Thus, $F_{\text{total}} = 128$ fN for our values $\kappa = 62$ fN, $s_T = 2.5/(\text{K}\mu\text{m})$, $\mathcal{D}_0 = 3.3$, and $r_0 = 22$ μm [35]. This force is eleven times larger than the force experienced in bulk by a DNA molecule of the same length, 83 kb, in a similar temperature gradient, 1 K/μm, Fig. 4(c) in [4]. In bulk, the molecule forms a bundle that

shields itself [4]. Stretching of the DNA eliminates shielding, see below.

Theory for Soret coefficient.—Paraphrasing the equilibrium thermodynamics theory for thermophoresis [4,7], we set $s_T = g'(T)/k_B T$, where g is Gibbs free energy per unit contour length of the solvent-DNA system. g is the sum of two [4] or four [7] terms. One term, g_{ion}, is due to the electrostatic energy in the double layer of ions surrounding a charged particle. It depends on the Debye length, $\lambda_D(T) = \sqrt{\epsilon(T) k_B T/2e^2 N_A I}$, where N_A is Avogadro's number and $\epsilon(T)$ is the dielectric constant of the solvent [4,7]. The other term is independent of λ_D when identified with the hydration entropy [4], and also, effectively, when modeled as in [7], see [7], Fig. S6.

The electrostatic energy g_{ion} is obtained by solving the Poisson-Boltzmann equation, often in the Debye-Hückel approximation valid for low surface potentials. For a cylinder, $g_{ion} \approx e^2\sigma_{eff}^2 \ln[1+\lambda_D/R_{DNA}]/4\pi\epsilon$ per unit length, with σ_{eff} the effective number of charges per unit length [25]. From this result, it follows that:

$$s_T^{(ion)} = g'_{ion}(T)/k_B T \approx \frac{\ell_B \sigma_{eff}^2}{T}\left(\beta \ln\left[1+\frac{\lambda_D}{R_{DNA}}\right] + \frac{1}{2}\frac{1-\beta}{1+\frac{R_{DNA}}{\lambda_D}}\right), \quad (7)$$

with $\beta = -(\epsilon' T/\epsilon) = 1.38$, $T = T_\infty + \Delta T_{max}/2 = 300$ K, and the Bjerrum length $\ell_B = e^2/(4\pi\epsilon k_B T) = 0.72$ nm. For our experimental conditions, the first, logarithmic term is at least a factor 10 larger than the second term.

Results for spheres which are valid for any thickness of the Debye layer [Eq. (12) in [36]], can be recast to a result for a cylinder, also valid for any Debye layer, supposedly,

$$s_T^{(ion,rod)} = \frac{\ell_B \sigma_{eff}^2}{T}\frac{\beta + (1+\beta)\frac{R_{DNA}}{2\lambda_D}}{(1+\frac{R_{DNA}}{\lambda_D})^2}. \quad (8)$$

Figure 4 shows fits to our experimental s_T values of these expressions plus a constant offset, $s_T^{(off)}$. The parameters of each fit are σ_{eff} and $s_T^{(off)}$. With n_{eff} the number of effective charges per base pair and $L_{bp} = 1.28 \times 0.34$ nm the length of a base pair after staining, $\sigma_{eff} = n_{eff}/L_{bp}$. The fits of the models in Eqs. (7) and (8), thus, return $n_{eff} = 0.14 \pm 0.07$, and $n_{eff}^{(rod)} = 0.2 \pm 0.1$, respectively. These values agree with the effective charge measured for DNA in bulk, $0.12e$/bp [4]. The offsets, $s_T^{(off)}$, are $(2.3 \pm 0.3)/(\mathrm{K}\mu\mathrm{m})$ and $(2.0 \pm 0.5)/(\mathrm{K}\mu\mathrm{m})$ for Eqs. (7) and (8), respectively.

Our results show that, at room temperature, the thermophoretic force on DNA is dominated by sources that are independent of the Debye length. The sum of such contributions is described by the offset $s_T^{(off)}$ [25]. This offset contains both ionic contributions (from, e.g., the Seebeck effect [7]) and nonionic contributions (from, e.g., solvation entropy or hydrophobicity [4]). This agrees with findings for protein solutions [37] but not with results for polystyrene beads [4] and micellar solutions [2]. For DNA in bulk, the thermophoretic force scales as $(\text{contour length})^{1/2}$ because of self-shielding [4]. DNA molecules shorter than their persistence length (~180 bp) cannot shield themselves, so from results in [4] obtained for such lengths, we find the Soret coefficient s_T per unit length of nonshielded DNA. Only a single ionic strength ($\lambda_D = 9.6$ nm) is considered in [4]. At that strength, 50 and 100 bp molecules yield $s_T = 3.3$ and $2.1/(\mathrm{K}\mu\mathrm{m})$, respectively, which averages to $(2.7 \pm 0.6)/(\mathrm{K}\mu\mathrm{m})$. We extrapolate our results in Fig. 4 to $\lambda_D = 9.6$ nm, using the fits of Eqs. (7) and (8). This gives $s_T = (3.0 \pm 0.4)$ and $(2.9 \pm 0.3)/(\mathrm{K}\mu\mathrm{m})$, respectively, in perfect agreement with $(2.7 \pm 0.6)/(\mathrm{K}\mu\mathrm{m})$ and twice more precise [25]. To the best of our knowledge, there are no other results we can compare with. Results for single-stranded DNA in bulk [38] seem irrelevant.

Discussion, conclusion, and perspectives.—Our experimental setup has some advantages: Localized heating in microfluidic devices can create convection, which will interfere with the measurements of the thermophoretic force [3]. Because of the small dimensions of the nanochannel and the modest temperature increase, $\Delta T_{max} \simeq 8$ K, convection does not occur in our device, Sec. 3.4 in [3]. The small dimensions of the nanochannel also prevent artifacts due to sedimentation [6] and interparticle interactions [2]. Moreover, the liquid surrounding the DNA is not heated directly with a laser, so there is no light pressure on the DNA as a potential source of error [3]. These advantages all vouch for the reliability of our data.

Our maximally simple model describes stretched DNA conformations perfectly with a single fitted parameter, s_T, which was measured this way. This supports our model and its s_T values. So does their agreement with values reported in [4] for DNA too short to shield itself. The weak-to-absent salt dependence of our s_T values supports the thermodynamic model for thermophoresis by being consistent with it.

Our temperature gradient of up to 1 K/μm stretches the central segment of DNA to 80% of its contour length. This extension exceeds all previously reported results obtained in nanochannels with similar dimensions and salt concentrations [39,40] and, hence, may be of practical interest: Research on genomic-length DNA confined inside nanofluidic structures has increased our understanding of biological interactions of DNA and enables coarse-grained optical mapping of the sequence of intact individual DNA molecules [41–46]. Stretching DNA to nearly its contour length remains a challenge, however. It requires either very narrow nanochannels [47,48], extreme salt concentrations [49], or crossed flows [46]. Very narrow channels are difficult both to fabricate and to load with DNA. Extreme salt concentrations are incompatible with biological conditions. And crossed flows require delicate balancing of the DNA in the flows. LILH, however, can stretch DNA up to 80% of its contour length in rather wide channels, at any salt

concentration, and in the absence of flows. By doing that, LILH can improve the optical resolution of local features on DNA, say for denaturation mapping [45] or for localization of interaction sites of proteins and enzymes [41,42].

This work was supported by the European Unions Seventh Framework Programme FP7/2007-2013 under Grants No. 201418 (READNA) and No. 278204 (CellOMatic), the Danish Council for Strategic Research Grant No. 10-092322 (PolyNano), the Danish Council for Independent Research—Natural Sciences (J. N. P.), and by Carlsbergfondet (J. N. P.).

*Present address: NIL Technology ApS, Diplomvej 381, DK-2800 Kongens Lyngby, Denmark.
†henrik.flyvbjerg@nanotech.dtu.dk.

[1] P. S. Epstein, Z. Phys. **54**, 537 (1929).
[2] R. Piazza and A. Guarino, Phys. Rev. Lett. **88**, 208302 (2002).
[3] S. Duhr, S. Arduini, and D. Braun, Eur. Phys. J. E **15**, 277 (2004).
[4] S. Duhr and D. Braun, Proc. Natl. Acad. Sci. U.S.A. **103**, 19678 (2006).
[5] S. Duhr and D. Braun, Phys. Rev. Lett. **96**, 168301 (2006).
[6] M. Braibanti, D. Vigolo, and R. Piazza, Phys. Rev. Lett. **100**, 108303 (2008).
[7] M. Reichl, M. Herzog, A. Götz, and D. Braun, Phys. Rev. Lett. **112**, 198101 (2014).
[8] H.-R. Jiang and M. Sano, Appl. Phys. Lett. **91**, 154104 (2007).
[9] R. Piazza and A. Parola, J. Phys. Condens. Matter **20**, 153102 (2008).
[10] R. D. Astumian, Proc. Natl. Acad. Sci. U.S.A. **104**, 3 (2007).
[11] A. Parola and R. Piazza, Eur. Phys. J. E **15**, 255 (2004).
[12] A. Parola and R. Piazza, J. Phys. Condens. Matter **17**, S3639 (2005).
[13] H. Brenner, Phys. Rev. E **74**, 036306 (2006).
[14] A. F. Andreev, Zh. Eksp. Teor. Fiz. **94**, 210 (1988) [Sov. Phys. JETP **67**, 117 (1988)].
[15] A. Würger, C. R. Mécanique **341**, 438 (2013).
[16] D. Braun and A. Libchaber, Phys. Rev. Lett. **89**, 188103 (2002).
[17] M. Ichikawa, H. Ichikawa, K. Yoshikawa, and Y. Kimura, Phys. Rev. Lett. **99**, 148104 (2007).
[18] H.-R. Jiang, H. Wada, N. Yoshinaga, and M. Sano, Phys. Rev. Lett. **102**, 208301 (2009).
[19] Y. T. Maeda, A. Buguin, and A. Libchaber, Phys. Rev. Lett. **107**, 038301 (2011).
[20] C. J. Wienken, P. Baaske, U. Rothbauer, D. Braun, and S. Duhr, Nat. Commun. **1**, 100 (2010).
[21] L. H. Thamdrup, N. B. Larsen, and A. Kristensen, Nano Lett. **10**, 826 (2010).
[22] The loading buffer consisted of 45 mM tris-base, 45 mM boric acid, and 1 mM Ethylenediaminetetraacetic acid (EDTA) (i.e., $0.05 \times$ Tris/Borate/EDTA, $I_{\mathrm{buf}} =$ 20 mM) with 3 vol% β-mercaptoethanol to suppress bleaching of YOYO-1 [23,40]. Under these conditions, the contour length of the DNA is $\ell_c = 72\ \mu$m after adjustment for stretching by the intercalating dye [24]. The ionic strength of the solution was varied by addition of NaCl at concentrations from 4 to 70 mM.
[23] W. Reisner, N. B. Larsen, H. Flyvbjerg, J. O. Tegenfeldt, and A. Kristensen, Proc. Natl. Acad. Sci. U.S.A. **106**, 79 (2009).
[24] K. Günther, M. Mertig, and R. Seidel, Nucleic Acids Res. **38**, 6526 (2010).
[25] See Supplemental Material at http://link.aps.org/supplemental/10.1103/PhysRevLett.113.268301 for temperature calibration, free energy calculation, density model, and alternative fits to data, which includes Refs. [26–32].
[26] O. Filevich and R. Etchenique, Anal. Chem. **78**, 7499 (2006).
[27] P. A. S. Jorge, C. Maule, A. J. Silva, R. Benrashid, J. L. Santos, and F. Farahi, Anal. Chim. Acta **606**, 223 (2008).
[28] M. H. Ulbrich and E. Y. Isacoff, Nat. Methods **4**, 319 (2007).
[29] D. Stigter, J. Colloid Interface Sci. **53**, 296 (1975).
[30] J. A. Schellman and D. Stigter, Biopolymers **16**, 1415 (1977).
[31] D. Stigter, Biopolymers **16**, 1435 (1977).
[32] K. I. Mortensen, L. S. Churchmann, J. A. Spudich, and H. Flyvbjerg, Nat. Methods **7**, 377 (2010).
[33] This is possible because $\mathcal{D}(x)$ remains somewhat larger than 1 in our experiments. Near $\mathcal{D}(x) = 1$, highly nonlinear elastic response is guaranteed, as it corresponds to fully stretched DNA.
[34] W. Reisner, J. P. Beech, N. B. Larsen, H. Flyvbjerg, A. Kristensen, and J. O. Tegenfeldt, Phys. Rev. Lett. **99**, 058302 (2007).
[35] For these values, $F_{\mathrm{total}} \to 146$ fN for $r_0 \to \infty$.
[36] Z. Wang, H. Kriegs, J. Buitenhuis, J. K. G. Dhont, and S. Wiegand, Soft Matter **9**, 8697 (2013).
[37] S. Iacopini and R. Piazza, Europhys. Lett. **63**, 247 (2003).
[38] P. Reineck, C. J. Wienken, and D. Braun, Electrophoresis **31**, 279 (2010).
[39] W. Reisner, K. J. Morton, R. Riehn, Y. M. Wang, Z. N. Yu, M. Rosen, J. C. Sturm, S. Y. Chou, E. Frey, and R. H. Austin, Phys. Rev. Lett. **94**, 196101 (2005).
[40] F. Persson, P. Utko, W. Reisner, N. B. Larsen, and A. Kristensen, Nano Lett. **9**, 1382 (2009).
[41] R. Riehn, M. C. Lu, Y. M. Wang, S. F. Lim, E. C. Cox, and R. H. Austin, Proc. Natl. Acad. Sci. U.S.A. **102**, 10012 (2005).
[42] Y. M. Wang, J. O. Tegenfeldt, W. Reisner, R. Riehn, X. J. Guan, L. Guo, I. Golding, E. C. Cox, J. Sturm, and R. H. Austin, Proc. Natl. Acad. Sci. U.S.A. **102**, 9796 (2005).
[43] J. T. Mannion and H. G. Craighead, Biopolymers **85**, 131 (2007).
[44] N. Douville, D. Huh, and S. Takayama, Anal. Bioanal. Chem. **391**, 2395 (2008).
[45] W. Reisner, N. B. Larsen, A. Silahtaroglu, A. Kristensen, N. Tommerup, J. O. Tegenfeldt, and H. Flyvbjerg, Proc. Natl. Acad. Sci. U.S.A. **107**, 13294 (2010).
[46] R. Marie, J. N. Pedersen, D. L. V. Bauer, K. H. Rasmussen, M. Yusuf, E. Volpi, H. Flyvbjerg, A. Kristensen, and K. U. Mir, Proc. Natl. Acad. Sci. U.S.A. **110**, 4893 (2013).
[47] H. Cao, J. O. Tegenfeldt, R. H. Austin, and S. Y. Chou, Appl. Phys. Lett. **81**, 3058 (2002).
[48] Q. Xia, K. J. Morton, R. H. Austin, and S. Y. Chou, Nano Lett. **8**, 3830 (2008).
[49] Y. Kim, K. S. Kim, K. L. Kounovsky, R. Chang, G. Y. Jung, J. J. dePablo, K. Jo, and D. C. Schwartz, Lab Chip **11**, 1721 (2011).